Absolute distance measurement of optically rough objects using asynchronous-optical-sampling terahertz impulse ranging

Takeshi Yasui,[1,2,*] Yasuhiro Kabetani,[1] Yoshiyuki Ohgi,[1] Shuko Yokoyama,[1,3] and Tsutomu Araki[1]

[1]Graduate School of Engineering Science, Osaka University, 1-3 Machikaneyama, Toyonaka, Osaka 560-8531, Japan

[2]Institute of Technology and Science, The University of Tokushima, 2-1 Minami-Josanjima, Tokushima 770-8506, Japan

[3]Micro-Optics Co. Ltd., 2-20 Oe-Nakayamacho, Nishikyoku, Kyoto 610-1104, Japan

*Corresponding author: yasui@me.tokushima-u.ac.jp

Received 23 June 2010; revised 21 August 2010; accepted 23 August 2010; posted 24 August 2010 (Doc. ID 130579); published 22 September 2010

We report on a real-time terahertz (THz) impulse ranging (IPR) system based on a combination of time-of-flight measurement of pulsed THz radiation and the asynchronous-optical-sampling (ASOPS) technique. The insensitivity of THz radiation to optical scattering enables the detection of various objects having optically rough surfaces. The temporal magnification capability unique to ASOPS achieves precise distance measurements of a stationary target at an accuracy of −551 μm and a resolution of 113 μm. Furthermore, ASOPS THz IPR is effectively applied to real-time distance measurements of a moving target at a scan rate of 10 Hz. Finally, we demonstrate the application of ASOPS THz IPR to a shape measurement of an optically rough surface and a thickness measurement of a paint film, showing the promise of further expanding the application scope of ASOPS THz IPR. The reported method will become a powerful tool for nondestructive inspection of large-scale structures.

OCIS codes: 110.6795, 120.0280, 280.3400, 280.5600.

1. Introduction

Recent progress made in the construction of large-scale structures on the scale from a few to several tens of meters, such as buildings, bridges, airplanes, ships, and parabolic antennae, increases the demand for precise distance and/or shape measurement techniques. One promising method to achieve noncontact distance measurement is to use an optical distance meter based on intensity-modulated continuous-wave (CW) light [1,2], ultrashort pulsed light [3,4], or an optical frequency comb [5,6]. For example, absolute distance measurement at a distance of 240 m is achieved with a resolution of 50 μm using the optical beat component between longitudinal modes of an optical frequency comb [5]. However, since most large-scale structures have optically rough surfaces, such as metal, plastic, rubber, or paint, optical scattering at their surfaces often hinders the use of optical distance meters. To avoid optical scattering and achieve specular reflection, a corner reflector has to be fixed on the target; however, this is an obstacle to attaining *in situ* distance measurement in open fields and shape measurement. One alternative approach for *in situ* measurement of optically rough objects is millimeter-wave or microwave radar, because the wavelengths used are much larger than the typical spatial dimensions of the surface roughness, making this technique insensitive to optical

0003-6935/10/285262-09$15.00/0

scattering. However, the precision of these radar devices is relatively low. For example, in conventional microwave and millimeter-wave radars [7–9], the measurement of the short range less than 10 m is extremely difficult. In short, the conventional distance measurement methods based on optical waves and electric waves have their own merits and demerits. Combining the merits of both methods would allow ideal distance measurement of optically rough objects to be achieved.

One potential electromagnetic wave combining the characteristics of both methods is terahertz (THz) radiation (0.1–10 THz frequency; 30–3000 μm wavelength) because it lies at the boundary between optical waves and electric waves and, hence, possesses characteristics of both [10]. Recently, pulsed THz radiation (THz pulses) has emerged as a new mode for sensing and imaging. Because the wavelength of THz radiation is still larger than the typical spatial dimensions of the surface roughness, insensitivity to optical scattering enables measurement of objects having optically rough surfaces. Furthermore, time-of-flight measurement of a reflected THz pulse, a technique known as THz impulse ranging (IPR) [11], possesses the possibility of realizing precise distance measurement because the pulse duration is extremely short, typically subpicoseconds to picoseconds. Therefore, THz IPR is highly promising for use in the precise distance measurement of optically rough objects, although pioneering work of THz IPR reports an application for a scale-model simulator of microwave radar [11].

However, when THz IPR is applied to these measurements, we are confronted with one technical difficulty: the requirement for mechanical stage scanning to produce a time delay due to the fact that detection of the THz pulses is based on pump–probe schemes in which a single mode-locked pulsed laser provides both the pump and the probe pulses. When we measure a target located at an unknown distance, scanning for the time delay has to be extended to the time period of the THz pulse train to ensure temporal overlapping between the THz pulse and the probe pulse. For example, to fully cover the THz pulse period of 12.2 ns used in the system presented here requires a mechanical stage with a scanning range of 1.83 m. If a conventional stepper motor-driven translation stage is used for this scanning, the measurement time will reach several tens of minutes, which will be a serious obstacle to practical adoption of THz IPR because the method is only applied to stationary objects. If THz IPR can be achieved in real time, the number of applications will be greatly increased, for example, moving targets and imaging measurement.

One effective method to realize rapid data acquisition of the temporal waveform is to use a rotary optical delay line equipped with fast rotating mirrors. A scan rate of up to 400 Hz and a time delay of up to 1 ns are demonstrated with this approach [12,13]. However, it is still difficult to cover the overall time period of the THz pulse train. Furthermore, there are several significant disadvantages, such as mechanical and acoustic vibrations of the fast rotating motor, spot size variations, and positional changes of the laser beam during scanning.

One promising method to achieve scanning with a rapid scan rate and long time delay at the same time is asynchronous optical sampling (ASOPS) using two mode-locked pulsed lasers with slightly mismatched mode-locked frequencies [14,15]. The ASOPS method enables us to linearly expand the time scale of ultrafast transient signals. The resulting slow signal to cover the overall time period can be captured directly on a standard oscilloscope without the need for mechanical time-delay scanning. Also, the ASOPS method can avoid the above-mentioned significant disadvantages inherent in the rotary optical delay line. Furthermore, this method always ensures temporal overlapping of the THz pulse and the probe pulse regardless of the difference of their optical path lengths because the period of the THz pulse is slightly detuned from that of the probe pulse. Therefore, it is no longer necessary to match the optical path lengths. Recently, the ASOPS method has been effectively applied to terahertz time-domain spectroscopy (TDS) to achieve rapid data acquisition and high spectral resolution at the same time [16–19]. However, other applications of the ASOPS method are still lacking in the THz region. Applying the ASOPS method to THz IPR will open the door for distance measurement of an optically rough object at an unknown distance in real time.

In the work described in this paper, we constructed a real-time THz IPR system based on the ASOPS method, which we call ASOPS THz IPR. We performed absolute displacement measurement of a stationary target and a moving one located at a distance within the range of several meters, which is the same order of magnitude as for large-scale structures. We further demonstrated a shape measurement of a stepped diffusing surface and a thickness measurement of a paint film to assess the effectiveness of this system as a nondestructive inspection tool for large-scale structures.

2. Principle of Operation

In the impulse ranging method based on time-of-flight measurement, the target distance is obtained from the time delay of a reflected pulse relative to a time-origin signal, which is independent of the target distance. In our ASOPS THz IPR system, a THz echo signal and a sum-frequency-generation (SFG) cross-correlation signal are used as the reflected pulse and the time-origin signal, respectively. Figure 1(a) shows a timing chart of the SFG signal and the THz echo signal, where ϕ is the time delay of the THz echo signal and T is the period of the SFG and THz pulse trains. Here, we define a spatial period of the THz pulse train L_{hsp} as follows:

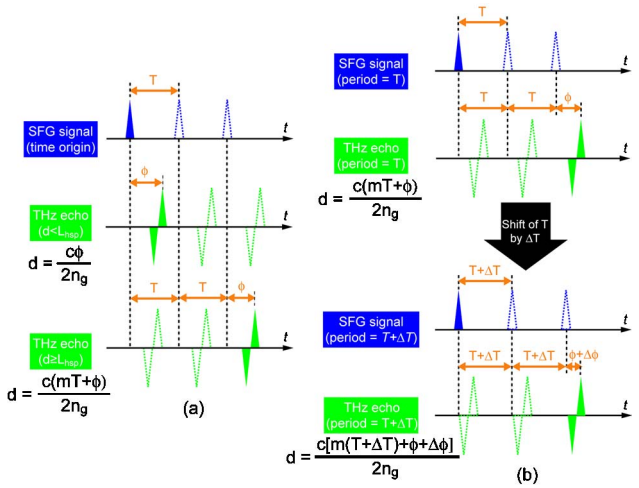

Fig. 1. (Color online) Principle of distance measurement. (a) Timing chart for SFG signal and THz echo signal when target distance d is shorter and longer than half of the spatial period L_{hsp} of a THz pulse train. (b) Timing chart for SFG signal and THz echo signal when the pulse period is set to T and $T+\Delta T$.

$$L_{\mathrm{hsp}} = \frac{cT}{2n_g}, \tag{1}$$

where n_g is the group refractive index of a medium for propagation of the THz pulse and c is the velocity of light in a vacuum. The n_g value is equal to 1 when the THz pulse propagates in air. When the target distance d is shorter than L_{hsp}, d is simply determined as follows [see the middle of Fig. 1(a)]:

$$d = \frac{c\phi}{2n_g}. \tag{2}$$

However, L_{hsp} of the THz pulse train is usually too short for ranging of a distant target. For example, when a THz pulse train with $T = 12.22\,\mathrm{ns}$, corresponding to a repetition frequency of 81.85 MHz, is used, as demonstrated in Section 4, L_{hsp} is only 1.833 m. If d exceeds L_{hsp}, we have to apply a modified equation

$$d = \frac{c(mT+\phi)}{2n_g}, \tag{3}$$

where m is the order of the measured THz pulse. For example, when $m = 2$, the timing chart of the THz echo signal is as illustrated in the lower part in Fig. 1(a). Because an oscilloscope or digitizer can measure only the time delay of the THz pulse relative to the SFG signal nearest in time, i.e., ϕ, we have to determine m and T for absolute distance measurement of a target at a distance over L_{hsp}. The period T can be obtained by measuring the laser output with a photodetector and a frequency counter. To determine m, T is changed by ΔT using a laser control system. Figure 1(b) shows the timing chart for the SFG signal and the THz echo signal when the pulse period is set to T and $T+\Delta T$. The change of T by ΔT results in a change of $\Delta\phi$ in the time delay ϕ. The target distance d before and after the change is given by

$$d = \frac{c(mT+\phi)}{2n_g} = \frac{c[m(T+\Delta T)+\phi+\Delta\phi]}{2n_g}. \tag{4}$$

Assuming that the target distance d is constant before and after the change of ΔT, ΔT and $\Delta\phi$ must satisfy the following relationship:

$$\Delta\phi = -m\Delta T. \tag{5}$$

Therefore, we can determine the order m by measuring ΔT and $\Delta\phi$.

3. Experimental Setup

We modify a transmission setup used in ASOPS THz TDS [16] into a reflection setup for ASOPS THz IPR. The experimental setup is shown in Fig. 2. We use two Kerr-lens mode-locked Ti:sapphire lasers for generation and detection of the THz pulse (pump and probe lasers). The individual mode-locked frequencies $f_1 (= 81.84746\,\mathrm{MHz})$ and $f_2 (= f_1 + 10\,\mathrm{Hz} = 81.84747\,\mathrm{MHz})$ of the two lasers, and the frequency difference between them $\Delta f (= f_2 - f_1 = 10\,\mathrm{Hz})$ are stabilized by two independent phase-locked loop control systems (PLL1 and PLL2). In the PLL electronics, the 150th harmonic component of the mode-locked frequency is filtered, amplified, and used to stabilize the mode-locked frequency using a piezoelectric transducer attached to an output coupler of the laser cavity. By using a rubidium (Rb) frequency standard (Rb FS; Stanford Research Systems FS725 with 10 MHz frequency, 5×10^{-11} accuracy, and 2×10^{-11} stability at 1 s) as a reference signal source for laser stabilization, the achieved instability of the mode-locked frequency is 2×10^{-11} at a gate time of 1 s. Precise control of f_1 and f_2 leads to

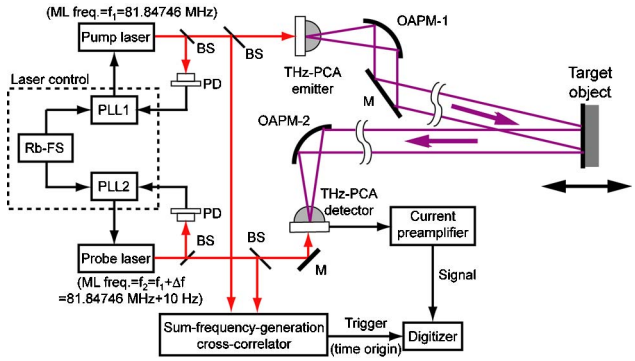

Fig. 2. (Color online) Experimental setup: pump and probe lasers, mode-locked Ti:sapphire lasers; PD, photodiodes; PLL1 and PLL2, phase-locked loop control systems; Rb FS, rubidium frequency standard; BS, beam splitter; THz PCA emitter, planar, large-area GaAs photoconductive antenna with an interdigitated electrode structure for THz generation; THz PCA detector, bowtie-shaped, low-temperature-grown GaAs photoconductive antenna for THz detection; OAPM-1 and OAPM-2, off-axis parabolic mirrors; M, plane mirror.

stabilization of Δf. The resulting timing jitter between the two lasers is suppressed to less than 400 fs, as discussed in Subsection 4.A.

Portions of the two laser beams are fed into an SFG cross correlator equipped with a nonlinear optical crystal by beam splitters, and the resulting SFG signal is used as the time origin for the ASOPS THz IPR measurement, which is independent of the target distance. The remaining parts of the two laser beams are incident on photoconductive antennas (PCAs) for THz generation and detection, namely, a THz PCA emitter and THz PCA detector, respectively. A planar, large-area GaAs PCA with an interdigitated electrode structure (Gigaoptics GmbH, Tera-SED 3) is used as the THz PCA emitter, whereas a bowtie-shaped, low-temperature-grown GaAs PCA (Hamamatsu Photonics; 1 mm bowtie length and a 5 μm gap) is used as the THz PCA detector. The THz pulse radiating from the THz PCA emitter is collimated by an off-axis parabolic mirror (OAPM-1) and then directed to a target object by a plane mirror (M). The THz pulse reflected at the surface of the object is collected and focused onto the THz PCA detector by another off-axis parabolic mirror (OAPM-2). To simulate the impulse ranging applications in open fields, the measurement is performed with humidity in normal atmosphere. The current signal from the THz PCA detector was amplified with a high-gain current preamplifier (AMP; 100 kHz bandwidth and 5×10^7 V/A sensitivity). The resulting voltage signal is measured at a scan rate of $\Delta f (= 10\,\text{Hz})$ with a fast digitizer (National Instruments, PCI-5122) by using the SFG signal as a trigger signal in the ASOPS THz IPR measurement.

4. Results

A. Distance Measurement of a Stationary Target

We first evaluated the basic performance of the ASOPS THz IPR system with a stationary target. A metal plate with a machined surface was placed at a distance of about 1 m. Figure 3 shows the temporal waveforms of the THz echo signal returned from the target; a measurement time of 10 s was required for signal integration of 100 temporal waveforms. The observed temporal profile was expanded by a temporal magnification factor of $f_1/\Delta f (= 81,847,460/10 = 8,184,746)$ according to the principle of the ASOPS method [16]. The upper and lower horizontal coordinates in Fig. 3 indicate, respectively, the *actual* time scale measured by the digitizer and the *real* time scale calibrated using the above magnification factor. Despite the optically rough surface, a temporal waveform of the pulsed THz radiation was measured at a good dynamic range due to the insensitivity of the THz radiation to optical scattering. Although the sample used has a machined surface with 10-point average roughness (R_{ZJIS}) of 1.03 μm and calculated average roughness (R_a) of 0.16 μm, the observed magnitude of the electric field was the same level as that when a metal mirror

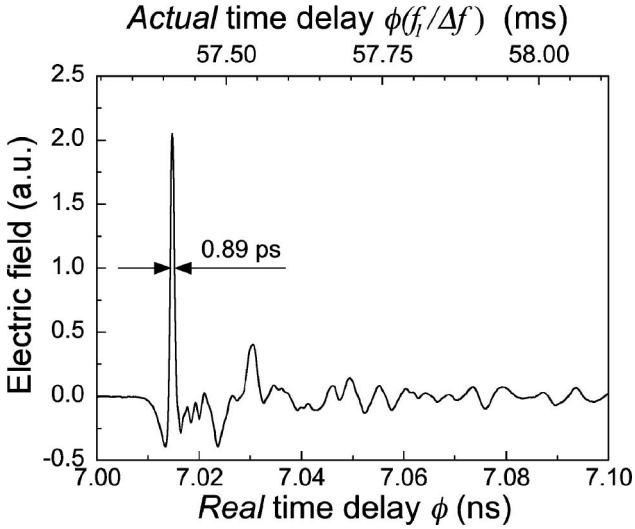

Fig. 3. Temporal waveforms of the THz echo signal returned from the machined surface of a metal plate. The upper and lower horizontal coordinates indicate the *actual* time scale measured by the digitizer and the *real* time scale calibrated using a temporal magnification factor of $f_1/\Delta f$, respectively.

($R_{\text{ZJIS}} = 0.06\,\mu$m and $R_a = 0.01\,\mu$m) was set as a sample (result not shown), indicating that the machined surface functions as a mirror for the THz pulse. The scattering effect of the THz wave on different surface roughness was investigated in detail elsewhere [20]. When the target position $\phi = 0$ ps was defined as a distance origin, the absolute distance d of the sample was determined to be 1.0522 m from the observed ϕ of 7.0147 ns using Eq. (2).

Here, let us consider the advantage when the ASOPS technique is applied for the impulse ranging method. In the conventional methods, the distance resolution and precision are largely limited by the response time of the receiver rather than the pulse duration of the source because the pulse duration usually exceeds the response time. For example, a response time of 100 ps limits the distance resolution to 30 mm even if a 1 ps pulse is used. To measure the temporal waveform of the pulse accurately without the limitation of the response time, we have to use the pump–probe scheme with mechanical time-delay scanning, resulting in a long measurement time. In this way, there is an inherent trade-off between the data acquisition speed and the distance precision in the conventional impulse ranging methods. On the other hand, the temporal magnification capability achieved by the ASOPS method resolves this trade-off issue by reducing the response time requirement of the receiver. For example, when the temporal magnification factor is set to 10^7, a 1 ps pulse signal is extended to a 10 μs pulse by the ASOPS method and, hence, can be accurately measured by a standard receiver having a response time of the order of nanoseconds or microseconds. In this case, a peak position precision of 0.1 μs in the *actual* time scale is equivalent to that of 10 fs in the *real* time scale, considering the temporal magnification factor of 10^7. Therefore,

the ASOPS method can achieve precise ranging in real time.

We next measured the displacement of a target located at a distance of about 1 m. The target was intermittently moved at intervals of 5 mm within a range of 200 mm by a translation stage. The black circle in Fig. 4 shows the relationship between the stage displacement and the measured displacement with the ASOPS THz IPR. A good linear relationship was confirmed between them. Discrepancy between them at each stage position is shown as the red triangle in Fig. 4. Because the displacement precision of the translation stage ($<1\,\mu$m) is much smaller than these discrepancies, the red point in Fig. 4 reflects the accuracy of the displacement measurement and, hence, the accuracy of distance measurement in ASOPS THz IPR. The mean accuracy in this demonstration was $-551\,\mu$m. We consider that this negative accuracy is caused by insufficient parallelism between the optical path of the THz beam and the moving direction of the translation stage.

In the distance measurement based on the ASOPS THz IPR, timing jitter between the pump and the probe lasers is a dominant factor in limiting the resolution of the distance measurement because the timing jitter causes the temporal magnification factor $f_1/\Delta f$ to fluctuate. Furthermore, the amount of timing jitter is dependent on the time delay ϕ between the THz pulse and the SFG signal [18]. To evaluate the effect of the timing jitter on the distance measurement, we measured the timing jitter of the THz pulse with respect to various ϕ values, as shown in Fig. 5. Here, the timing jitter was defined as the standard deviation of the temporal position of the positive signal peak in 100 repeated single-sweep measurements of the THz echo signal. The maximum timing jitter was 383 fs at $\phi = 12$ ns. The axis of the distance resolution estimated from the timing jitter is indicated at the right vertical coordinate in Fig. 5. Therefore, distance measurement could be achieved

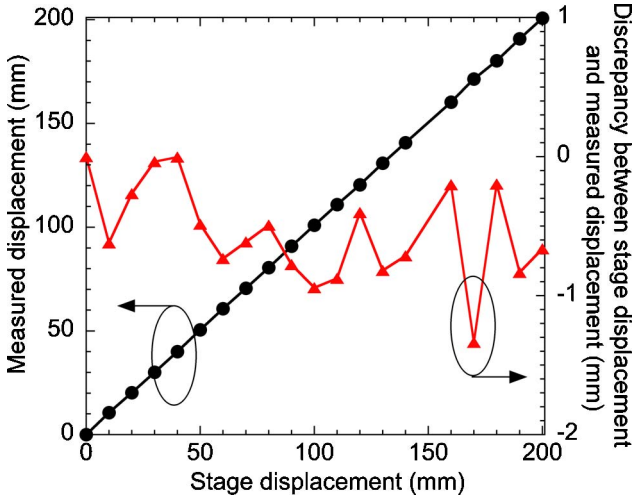

Fig. 4. (Color online) Relationship between stage displacement and measured displacement (black circle) and discrepancy between them (red triangle).

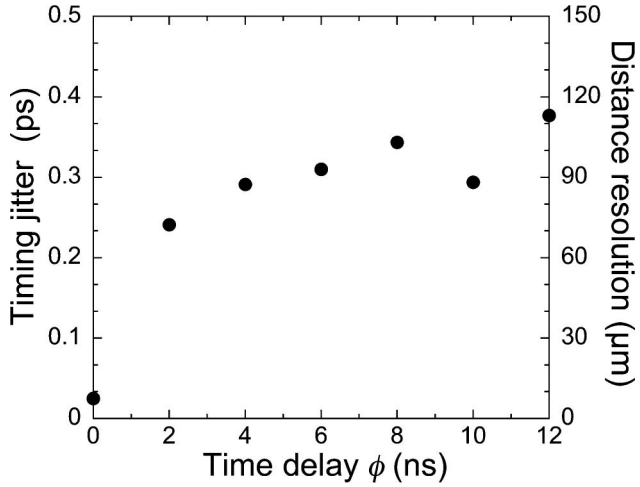

Fig. 5. Relationship between time delay ϕ and timing jitter. Distance resolution calculated by the timing jitter is given at the right vertical coordinate.

within the distance resolution of $113\,\mu$m by the present ASOPS THz IPR system.

We next determined the absolute distance of a metal plate located at a distance greater than half of the spatial period L_{hsp} of 1.833 m. The target was a metal plate placed at an unknown distance greater than 1.833 m. When the initial T was set to 12.21785 ns, the temporal waveform of the THz echo pulse was observed as the upper blue curve in Fig. 6. At this target position, the time positions of the peaks in the

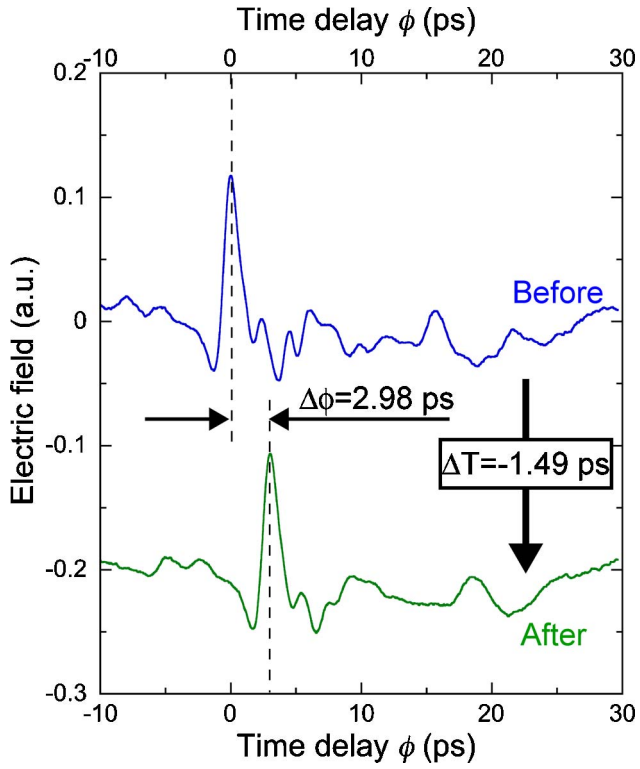

Fig. 6. (Color online) Absolute distance measurement of the target located at a distance greater than L_{hsp}. The temporal waveform after shift of T (lower green curve) is offset for clarity.

SFG signal and the THz echo signal temporally overlapped, indicating that $\phi = 0$ ps. Then, T was shifted by -1.49 ps$(= \Delta T)$. The resulting THz echo signal is shown as the lower green curve in Fig. 6. This shift caused a change in ϕ of 2.98 ps$(= \Delta\phi)$. Therefore, the order m of the measured THz pulse was calculated to be 2 based on Eq. (5). To avoid ambiguities when determining the m value, the precision to determine the temporal position of the THz pulse peak should be much better than $\Delta\phi$. The actual precision in the present system was limited to within 0.383 ps by the timing jitter between the two lasers (see Fig. 5). Therefore, the absolute distance was correctly determined in this demonstration that $\Delta\phi = 2.98$ ps. To determine the absolute distance without the ambiguities of the m value, the ΔT value should be set by considering the precision of the peak determination. Finally, we determined the target distance to be 3.6629 m based on Eq. (3). This value is in good agreement with the actual distance measured with a scale.

The main limiting factor for long distance measurement is THz absorption caused by the atmospheric water vapor because it attenuates and distorts the temporal waveform of the pulsed THz radiation. Here, we estimate the maximum measurable distance in the present system. When DR is defined as the ratio of the maximum magnitude of amplitude in the presence of the THz beam to standard deviation of amplitude in the absence of the THz beam [21], the present system achieved a DR of 377 at the acquisition time of 10 s (see Fig. 3). On the other hand, attenuation of the THz wave in the atmosphere depends on the weather and THz frequency. For example, in the case of sunny weather, the attenuation is 100 dB/km at the frequency of 0.5 THz [22]. When the sample has a flat, smooth surface for the THz wave and is adjusted to be at a good incident angle, most of the THz pulse will be retuned to the THz PCA detector as specular reflection, as shown in Fig. 3. Under these conditions, when the maximum measurable distance is defined as a distance that the DR is equal to 2, it is estimated to be 228 m at the acquisition time of 10 s. However, if the sample has a tilted, uneven, or bent surface, the collection efficiency of the reflected THz pulse with the THz PCA detector will largely decrease due to the specular reflection. In this case, mechanical scanning of the THz beam or phased array antenna will be required. Furthermore, diffraction of the THz beam during the long propagation will decrease the collection efficiency.

B. Distance Measurement of a Moving Target

To evaluate the real-time measurement capability of the ASOPS THz IPR, we measured the distance of a moving target in real time. The target was a metal plate placed at a distance of about 1 m. Then, the target was continuously moved by 200 mm at a speed of 25 mm/s using a translation stage. Figure 7 illustrates the results of six consecutive temporal waveforms of the THz echo signal acquired in a single-sweep measurement; the lower horizontal scale indicates the time delay ϕ between the THz echo signal and the SFG signal. In this case, the absolute distance d of the sample was calculated from Eq. (2) [see the middle of Fig. 1(a)] and is indicated on the upper horizontal coordinate in Fig. 7. When a target position indicating $\phi = 0$ ps was defined as the distance origin, the initial distance of the moving target was determined to be 1.035 m. The temporal change of the THz echo signal is shown as a movie in Media 1, indicating that the moving target is continuously approaching the distance origin.

In this demonstration, an acquisition time of 100 ms was required to scan the time window of 12.22 ns, although Fig. 7 indicates only a part of the whole time window to be measured. If a stepper-motor-driven translation stage with a moving speed of 1 mm/s is used for this time-delay scanning, the measurement time will reach 1833 s. Therefore, the measurement time achieved by the ASOPS method is 4 orders of magnitude shorter than that achieved by the conventional mechanical-time-delay method. We next compare the DR of the pulsed THz electric field between the ASOPS and the conventional

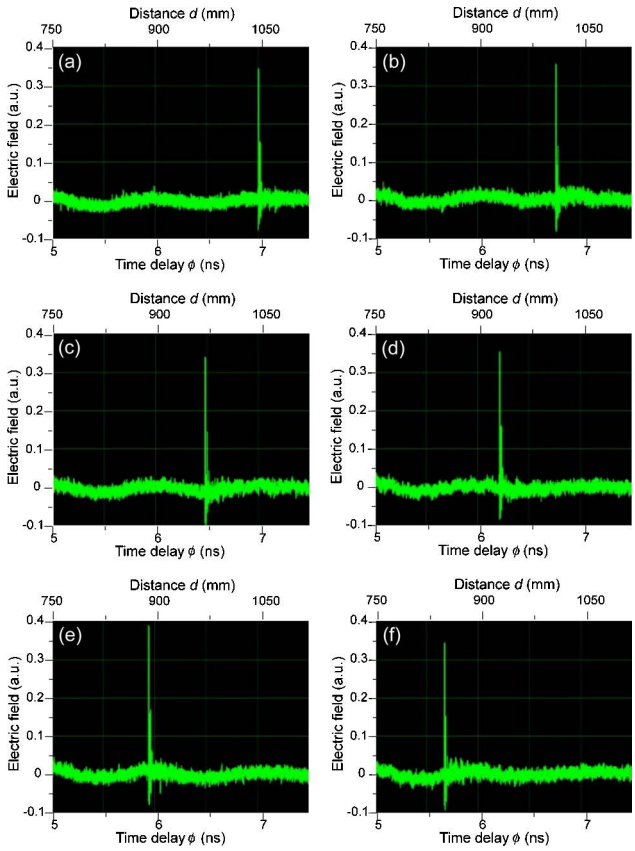

Fig. 7. (Color online) Six consecutive measurements of the THz echo signal when a target was continuously moved by 200 mm at a speed of 25 mm/s using a translation stage (Media 1). The lower horizontal coordinate indicates the time delay ϕ between the THz echo signal and the SFG signal. The target distance d determined from ϕ is given at the upper horizontal scale.

mechanical-time-delay methods. The DR of the THz temporal waveforms in Fig. 7 was 32. One may feel that the DR of these THz signals is very low compared with the conventional mechanical-time-delay method. However, there is a large difference in measurement time between the two methods. Because the DR of the electric field is proportional to the square root of the measurement time in the ASPOS method [17], the DR in the present system (= 32 at a measurement time of 100 ms) is comparable to that in the conventional mechanical-time-delay method (typically, a DR = 1000 at a measurement time of 100 s). Furthermore, it should be emphasized that this DR is maintained at any temporal position in the time window of 12.22 ns, which is technically difficult in the conventional method due to the slow acquisition time.

Here, let us consider the distance resolution and the maximum detectable speed when the target is unidirectionally moved at a constant speed along the propagation direction of the THz beam. In this case, the distance resolution is limited by the relationship between the sample speed and the scan rate of the measurement because the target distance changes between one scan and the next scan. Figure 8 shows the relationship between the sample speed and the distance resolution with respect to three different scan rates of 10 Hz (red solid line), 100 Hz (blue dotted line), and 1000 Hz (green broken line). The distance resolution increases in proportion to the increase of the sample speed or the decrease of the scan rate. In the case of the demonstration in Fig. 7 and Media 1, the distance resolution was 2.5 mm. On the other hand, when the distance resolution exceeds half of the spatial period of the THz pulse train $L_{\mathrm{hsp}}(= 1.833\,\mathrm{m})$ by increasing the sample speed, the target distance can no longer be determined. Therefore, the sample speed gives the maximum detectable speed of the moving target. The maximum detectable speed at a scan rate of 10 Hz was 18.33 m/s(= 65.99 km/h). The higher scan rate of the measurement is important in measuring the distance of a faster-moving target at high resolution. Although the scan rate in the present system was limited to 10 Hz by the electrical bandwidth of the current preamplifier (= 100 kHz) and the actual spectral bandwidth of the pulsed THz radiation (= 1 THz), it should be possible to further increase Δf by using a faster THz detector and/or higher-repetition-rate mode-locked lasers [17,18].

C. Shape Measurement of a Stepped Object

The real-time measurement capability of the ASOPS THz IPR system enables us to expand its scope to imaging applications. Next, we demonstrate the surface shape measurement of a stepped metal object. A schematic drawing of the stepped object is shown in Fig. 9(a). The THz beam was unidirectionally scanned across the steps by moving the object with a translation stage. Figure 9(b) shows the temporal waveforms of the THz echo signal measured at five different steps on the object. Also, the temporal behavior of the THz echo signal is shown as a movie in Media 2. The change of the THz echo signals clearly reflected the surface shape of the object under test. The transverse resolution in this demonstration would be equal to a diameter of the THz beam (= 20 mm) if the diffraction of the THz beam during the propagation is negligible. The reason we used an unfocused THz beam is that it is difficult to apply an imaging system with a fixed focal length for a sample located at an unknown distance. If an automatic focusing system of the THz beam is used for such a sample, the transverse resolution will be improved to less than a few millimeters.

In this demonstration, it is important to note that the ASOPS THz IPR can easily achieve remote measurement of the object shape without knowledge of the object distance because it is unnecessary to match the optical path lengths between the THz

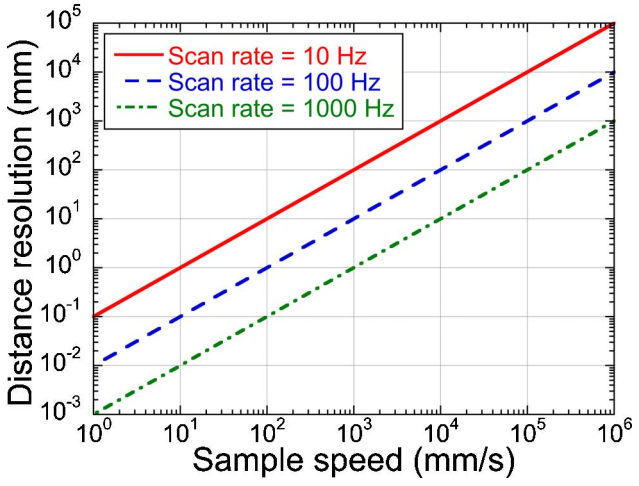

Fig. 8. (Color online) Relationship between the sample speed and the distance resolution with respect to three different scan rates of 10 Hz (red solid line), 100 Hz (blue dotted line), and 1000 Hz (green broken line).

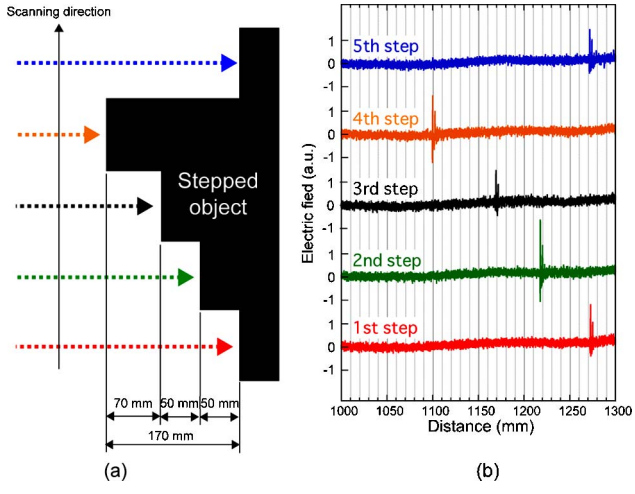

Fig. 9. (Color online) Shape measurement of a stepped metal object: (a) schematic drawing of the object and scanned THz beam and (b) temporal waveform of the THz echo signal measured at five different steps on the object (Media 2).

pulse and the probe pulse. Therefore, the ASOPS THz IPR will be a powerful tool for real-time profilometry of industrial products moved on a conveyor belt.

D. Thickness Measurement of Paint Film

From the viewpoint of maintenance inspection of large-scale structures, there is also considerable need to detect delamination of paint films on metal substrates, which is an important problem in practice due to the fact that metal substrates exhibit corrosion resulting from moisture or salt penetration through areas where paint has peeled off. Although tap testing is normally used for such an inspection, maintenance workers are exposed to the risk of falling from large-scale structures during this work. Unfortunately, since paint films are usually opaque and cause strong scattering and/or absorption of visible and infrared light, it is difficult to apply optical probe methods for this purpose. In contrast, since THz radiation highly penetrates dry, nonmetallic, nonpolar materials, it is suitable for remote nondestructive inspection of paint films based on THz tomography [23]. A device based on this technique, called a THz paintmeter, is reported [24–26]; however, conventional THz paintmeters can be applied only to targets located at a known distance due to the limited time window in the mechanical time-delay scanning [24,25] or electro-optical time-to-space conversion [26]. Therefore, long-distance THz paintmeters are another interesting application of the ASOPS THz IPR.

We demonstrated thickness measurement of a single-layer paint film using the ASOPS THz IPR system. As a sample, we used an oil-based, alkyd paint film (white color) on an aluminum substrate located at a distance of about 1 m. The group refractive index in the THz region n_g, geometric thickness D, and optical thickness n_gD of the paint film were determined in advance to be 2.59, 220 μm, and 570 μm, respectively, using a conventional THz paintmeter equipped with mechanical time-delay scanning [24], and a contact-type thickness meter (eddy-current type, precision $\pm 3\%$ of the actual thickness). Figure 10(a) shows an original signal of the THz echo pulse for the single-layer paint film; however, it is a little difficult to distinguish the first from the second THz echo signals accurately, which come from the air/paint (paint surface) and paint/substrate (paint back surface) interfaces, respectively. We next calculated an impulse response signal of the THz echo pulse as shown in Fig. 10(b), based on numerical Fourier deconvolution [23]. As a result, we confirmed that two THz echo signals were separated by 3.8 ps. The time separation Δt between the two echoes is given by

$$\Delta t = \frac{2n_gD}{c}. \tag{6}$$

Therefore, the geometric thickness D of the paint film was determined to be 205 μm from Δt of 3.8 ps and n_g of 2.59. There was a discrepancy of 7% between this result and the result obtained with the contact-type thickness meter. Considering that the measurement spot in the ASOPS THz IPR is not completely consistent with those measured with the conventional THz paintmeter and the contact-type thickness meter, and that the paint sample prepared by us indicates an uneven thickness distribution of about 10% [24,25], this discrepancy was within the estimated uncertainty. The minimum detectable thickness of the paint film is limited to 51.5 μm by the pulse duration of 0.89 ps (see Fig. 3) and the n_g value of 2.59 of the paint film [24]. If the n_g value of the paint film is unknown, one can determine only the optical thickness n_gD from Eq. (6). It should be possible to apply the ASOPS THz IPR to detection and two-dimensional mapping of areas where paint has peeled off, as demonstrated with the previous THz paintmeter [24].

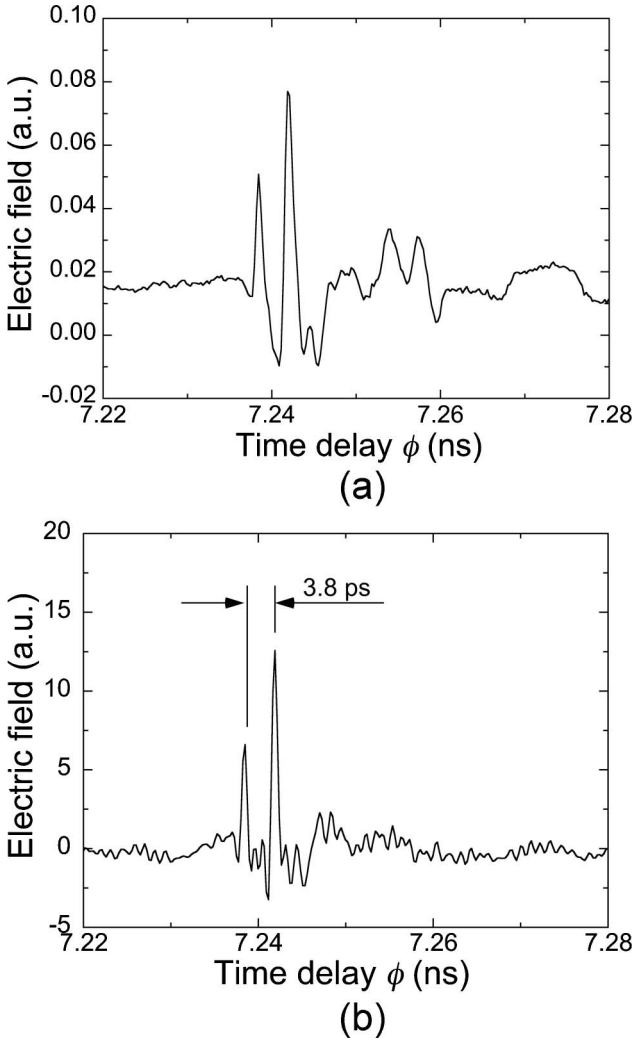

Fig. 10. (a) Original signal and (b) impulse response signal of THz echo pulse returned from a single-layer paint film on an Al plate.

5. Conclusions

We constructed an ASOPS THz IPR system combining the advantages of both optical distance meters

and electric-wave radars. The insensitivity of THz radiation to optical scattering enables detection of various objects having optically rough surfaces. Combination of time-of-flight measurement using an 0.89 ps THz pulse with temporal magnification capability achieved by the ASOPS method was used for distance measurement of a stationary target at an accuracy of $-551\,\mu$m and a resolution of $113\,\mu$m. Although the achieved ranging performance could not go beyond that in the optical distance meter [5], the proposed method has the big advantage of the *in situ* distance measurement of optically rough objects over the optical distance meters due to insensitivity to optical scattering. We proposed a unique method to determine the absolute distance of a target located at a distance in excess of half of the spatial period of the THz pulse train ($= 1.833$ m). Furthermore, the ASOPS THz IPR system was effectively applied to real-time distance measurement of a moving target at a scan rate of 10 Hz. Finally, we demonstrated the application of the ASOPS THz IPR system to shape measurement of an optically rough surface and thickness measurement of a paint film, showing the potential to further expand the application scope of the THz IPR method. The ASOPS THz IPR has the potential to become a powerful tool for nondestructive inspection of large-scale structures if the system can be made more compact, robust, flexible, and cost effective by use of a fiber-laser-based ASOPS system [16] and fiber-coupled PCAs [27].

This work was supported by Grants-in-Aid for Scientific Research, 20560036 and 21650111, from the Ministry of Education, Culture, Sports, Science, and Technology of Japan. We also gratefully acknowledge financial support from Renovation Center of Instruments for Science Education and Technology of Osaka University, Japan.

References

1. I. Fujima, S. Iwasaki, and K. Seta, "High-resolution distance meter using optical intensity modulation at 28 GHz," Meas. Sci. Technol. **9**, 1049–1052 (1998).
2. K. Seta, T. Oh'ishi, and S. Seino, "Optical distance measurement using inter-mode beat of laser," Jpn. J. Appl. Phys. **24**, 1374–1375 (1985).
3. J. Ye, "Absolute measurement of a long, arbitrary distance to less than an optical fringe," Opt. Lett. **29**, 1153–1155 (2004).
4. I. Coddington, W. C. Swann, L. Nenadovic, and N. R. Newbury, "Rapid and precise absolute distance measurements at long range," Nat. Photon. **3**, 351–356 (2009).
5. K. Minoshima and H. Matsumoto, "High-accuracy measurement of 240 m distance in an optical tunnel by use of a compact femtosecond laser," Appl. Opt. **39**, 5512–5517 (2000).
6. S. Yokoyama, T. Yokoyama, Y. Hagihara, T. Araki, and T. Yasui, "A distance meter using a terahertz intermode beat in an optical frequency comb," Opt. Express **17**, 17324–17337 (2009).
7. D. L. Maskell and G. S. Woods, "A frequency modulated envelope delay FSCW radar for multiple-target applications," IEEE Trans. Instrum. Meas. **49**, 710–715 (2000).
8. M. Mitsumoto, N. Uehara, S. Inatsune, and T. Kirimoto, "Target distance and velocity measurement algorithm to reduce false target in FMCW automotive radar," IEICE Trans. Commun. **E83-B**, 1983–1989 (2000).
9. G. A. Ybarra, S. H. Ardalan, C. P. Hearn, R. E. Marshall, and R. T. Neece, "Detection of target distance in the presence of an interfering reflection using a frequency-stepped double sideband suppressed carrier microwave radar system," IEEE Trans. Microwave Theory Tech. **39**, 809–818 (1991).
10. M. Tonouchi, "Cutting-edge terahertz technology," Nat. Photon. **1**, 97–105 (2007).
11. R. A. Cheville and D. Grischkowsky, "Time domain THz impulse ranging studies," Appl. Phys. Lett. **67**, 1960–1962 (1995).
12. J. Xu and X.-C. Zhang, "Circular involute stage," Opt. Lett. **29**, 2082–2084 (2004).
13. J. Kim, S.-G. Jeon, J.-I. Kim, and Y.-S. Jin, "Terahertz pulse detection using rotary optical delay line," Jpn. J. Appl. Phys. **46**, 7332–7335 (2007).
14. P. A. Elzinga, R. J. Kneisler, F. E. Lytle, Y. Jian, G. B. King, and N. M. Laurendeau, "A pump/probe method for fast analysis of visible spectral signatures utilizing asynchronous optical sampling," Appl. Opt. **26**, 4303–4309 (1987).
15. Y. Takagi and S. Adachi, "Subpicosecond optical sampling spectrometer using asynchronous tunable mode-locked lasers," Rev. Sci. Instrum. **70**, 2218–2224 (1999).
16. T. Yasui, E. Saneyoshi, and T. Araki, "Asynchronous optical sampling terahertz time-domain spectroscopy for ultrahigh spectral resolution and rapid data acquisition," Appl. Phys. Lett. **87**, 061101 (2005).
17. A. Bartels, A. Thoma, C. Janke, T. Dekorsy, A. Dreyhaupt, S. Winnerl, and M. Helm, "High-resolution THz spectrometer with kHz scan rates," Opt. Express **14**, 430–437 (2006).
18. A. Bartels, R. Cerna, C. Kistner, A. Thoma, F. Hudert, C. Janke, and T. Dekorsy, "Ultrafast time-domain spectroscopy based on high-speed asynchronous optical sampling," Rev. Sci. Instrum. **78**, 035107 (2007).
19. T. Yasui, M. Nose, A. Ihara, K. Kawamoto, S. Yokoyama, H. Inaba, K. Minoshima, and T. Araki, "Fiber-based, hybrid terahertz spectrometer using dual fiber combs," Opt. Lett. **35**, 1689–1691 (2010).
20. R. F. Anastasi and E. I. Madaras, "Terahertz NDE for metallic surface roughness evaluation," in *Proceedings of 4th International Workshop on Ultrasonic and Advanced Methods for Nondestructive Testing and Material Characterization*, C. H. Chen, ed. (NDT.net, 2006), pp. 57–62.
21. M. Naftaly and R. Dudley, "Methodologies for determining the dynamic ranges and signal-to-noise ratios of terahertz time-domain spectrometers," Opt. Lett. **34**, 1213–1215 (2009).
22. H. J. Liebe, "Atmospheric water vapor: a nemesis for millimeter wave propagation," in *Atmospheric Water Vapor*, A. Deepak, Th. D. Wilkerson, and L. H. Ruhnke, eds. (Academic, 1980), pp. 143–201.
23. D. M. Mittleman, S. Hunsche, L. Boivin, and M. C. Nuss, "T-ray tomography," Opt. Lett. **22**, 904–906 (1997).
24. T. Yasui, T. Yasuda, K. Sawanaka, and T. Araki, "A terahertz paintmeter for non-contact monitoring of thickness and drying progress in paint film," Appl. Opt. **44**, 6849–6856 (2005).
25. T. Yasuda, T. Iwata, T. Araki, and T. Yasui, "Improvement of minimum paint film thickness for THz paintmeters by multiple regression analysis," Appl. Opt. **46**, 7518–7526 (2007).
26. T. Yasuda, T. Yasui, T. Araki, and E. Abraham, "Real-time two-dimensional terahertz tomography of moving objects," Opt. Commun. **267**, 128–136 (2006).
27. B. Sartorius, H. Roehle, H. Künzel, J. Böttcher, M. Schlak, D. Stanze, H. Venghaus, and M. Schell, "All-fiber terahertz time-domain spectrometer operating at 1.5 μm telecom wavelengths," Opt. Express **16**, 9565–9570 (2008).